Histochemistry and Cell Biology (2020) 153:185–192
https://doi.org/10.1007/s00418-019-01834-z

SHORT COMMUNICATION

RNAscope dual ISH–IHC technology to study angiogenesis in diffuse large B-cell lymphomas

Tiziana Annese[1] · Roberto Tamma[1] · Michelina De Giorgis[1] · Simona Ruggieri[1] · Eugenio Maiorano[2] · Giorgina Specchia[3] · Domenico Ribatti[1]

Accepted: 6 December 2019 / Published online: 13 December 2019

Abstract

Diffuse large B-cell lymphomas (DLBCLs) are the most common types of Non-Hodgkin's lymphomas and are highly heterogeneous in terms of phenotype and treatment response. The natural course of DLBCLs tumor progression is featured by a flow of events leading to the enhancement of proliferative and invasive capabilities and, therefore, towards the establishment of a more aggressive phenotype. Angiogenesis is a constant hallmark of DLBCLs progression, has prognostic potential and promote DLBCLs dissemination. The study of DLBCLs angiogenesis mechanisms, and the tumor endothelium characterization, will allow us to identify new prognostic/predictive biomarkers to proper patient selection to antiangiogenic treatment. In our previous work, by RNAscope technology, we have demonstrated that Janus kinase (Jak) and signal transducer activator of transcription pathway (STAT) is one of the proangiogenic pathways activated in DLBCLs and it drives neoangiogenesis occurred by vasculogenesis mechanism. Here, we describe a detailed protocol to perform RNAscope technology alone and in combination with immunohistochemistry (called dual RNAscope ISH–IHC) in DLBCLs formalin-fixed, paraffin-embedded sections. We propose dual ISH–IHC as an extremely powerful method to study angiogenesis in DLBCLs, because it allows one to answer important biological questions that are difficult to address using other single methods.

Keywords RNAscope · Dual ISH–IHC · Angiogenesis · STAT3 · Diffuse large B-cell lymphomas

Abbreviations

ACD	Advanced cell diagnostics
DLBCLs	Diffuse large B-cell lymphomas
ECs	Endothelial cells
FFPE	Formalin-fixed paraffin-embedded
FVIII	Coagulation factor VIII
IHC	Immunohistochemistry
ISH	In situ hybridization
min	Minute/minutes
NHLs	Non-Hodgkin lymphomas
on	Overnight
R-CHOP	Rituximab, cyclophosphamide, doxorubicin, vincristine and prednisone
RT	Room temperature
sec	Seconds
STAT3	Signal transducer and activator of transcription 3
TAM	Tumor-associated macrophages

✉ Domenico Ribatti
domenico.ribatti@uniba.it

Tiziana Annese
tiziana.annese@uniba.it

Roberto Tamma
roberto.tamma@uniba.it

Michelina De Giorgis
michelina.degiorgis@uniba.it

Simona Ruggieri
simona.ruggieri@uniba.it

Eugenio Maiorano
eugenio.maiorano@uniba.it

Giorgina Specchia
giorgina.specchia@uniba.it

[1] Department of Basic Medical Sciences, Neurosciences and Sensory Organs, Section of Human Anatomy and Histology, University of Bari Medical School, Piazza Giulio Cesare, 11 Policlinico, 70124 Bari, Italy

[2] Department of Emergency and Organ Transplantation, Operating Unit of Pathological Anatomy, Aldo Moro University, Bari, Italy

[3] Department of Emergency and Organ Transplantation (D.E.T.O.), Hematology Section, University of Bari, Bari, Italy

TRR Target retrieval reagent
WB Washing buffer

Introduction

Diffuse large B-cell lymphomas (DLBCLs), with an incidence of 30%, are the most common types of Non-Hodgkin's lymphomas (NHLs), and are highly heterogeneous in terms of phenotype and treatment response (Jaffe et al. 2008; Khosravi Shahi and Perez Manga 2006). Based on morphological differences and gene expression profiles, DLBCLs are classified in activated B-cell-like (ABC) and germinal center B-cell-like (GCB) subtypes, associated with different prognoses with the same common treatment. First-line ABC and GCB common treatment is R-CHOP21 (rituximab, cyclophosphamide, doxorubicin, vincristine and prednisone) every 21 days for six cycles (Feugier et al. 2005). Although a significantly improved survival was attributed to R-CHOP treatment, a high number of patients remain refractory to this first-line chemotherapy or experience relapse, with a resulting poor outcome (Coiffier and Sarkozy 2016). Therefore, in addition to immuno-chemotherapy, targeted-therapy, radiation-therapy and blood stem cell transplant have been developed as second/third-line therapies to improve DLBCLs treatment outcome (Friedberg 2011).

As for most tumors, the natural course of DLBCLs is characterized by tumor progression, featured by a flow of events leading to the enhancement of proliferative and invasive capabilities, toward the establishment of a more aggressive phenotype (Cacciatore et al. 2012). DLBCLs progression is the result of an articulated mechanism which requires the constant crosstalk between tumor cells and the faulty surrounding microenvironment that promotes tumor survival and expansion, local invasion/spreading, and escape from the immunological response (Ungefroren et al. 2011). Microenvironment cells, such as fibroblasts, endothelial cells, mast cells, tumor-associated macrophages and lymphocytes, release angiogenic growth factors and cytokines, and angiogenesis are a constant hallmark of DLBCLs progression, have prognostic potential and promote DLBCLs dissemination (Ribatti et al. 2013). The study of DLBCLs angiogenesis mechanisms, with the tumor endothelium characterization, will allow us to identify new prognostic/predictive biomarkers to proper patient selection to antiangiogenic treatment as first-line therapy.

It is known that the Janus kinase (JAK) and signal transducer activator of transcription (STAT) pathways are involved in NHLs, and a high nuclear expression of STAT3 is associated with unfavorable prognosis in DLBCLs (Pan et al. 2018; Wu et al. 2011). In our previous work, we have also demonstrated a higher STAT3 mRNA expression in ABC compared with GCB by RNAscope technology, moreover, we have demonstrated that ABC blood vessels are lined by $FVIII^+/STAT3^+$ endothelial cells, underlying that neoangiogenesis occur by vasculogenesis mechanism (Tamma et al. 2019).

RNAscope technology is a new cutting edge in situ hybridization (ISH) technology based on probe design strategy that enables simultaneous signal amplification and background noise suppression, patented by advanced cell diagnostics (ACD). By RNAscope technology, it is possible to detect even small amounts of RNA at resolution level of single probe visualization in individual cells. The RNAscope approach can be used with archival formalin-fixed and paraffin-embedded (FFPE) tissue samples on glass slides, and the stained slides can be visualized under standard bright-field microscope, fluorescent microscope, or laser confocal scanning microscope depending on the type of colorimetric detection used (Wang et al. 2012). The newest approaches are based on the association of ISH and immunohistochemistry (IHC), called dual RNAscope ISH–IHC, a powerful technique allowing the integration of molecular information with histopathology for optimal clinical interpretation. The RNAscope technology is the perfect assay to evaluate, with high sensitivity and specificity, the gene expression in situ in routine clinical specimen types in combination with IHC.

In this study, working on human formalin-fixed paraffin-embedded (FFPE) biopsies of patients diagnosed with DLBCLs, we applied, on the same sections, ISH for the STAT3 mRNA detection by RNAscope, in combination with FVIII protein expression by immunohistochemistry. We show detailed and extensive protocols, with tricks, to perform STAT3 RNAscope and STAT3/FVIII dual RNAscope ISH–IHC on DLBCLs, and we indicate how to scan and analyze the slides by Aperio ScanScope CS and by Trainable Weka Segmentation plugin of Fiji, respectively. We propose RNAscope dual ISH–IHC as an extremely powerful method to study angiogenesis in DLBCLs, because it allows one to answer important biological questions concerning angiogenesis mechanisms and endothelium features that are difficult to address using other single methods.

Materials and methods

Patients

Tissue samples from patients diagnosed with DLBCLs were collected from the archive of the Section of Pathology of the University of Bari, Hospital Policlinico, Bari, Italy. All procedures were in accordance with the institutional and national ethical standards and signed informed consent from individual patients were obtained to conduct the study. All patients had pathologically confirmed DLBCLs.

STAT3 RNAscope protocol on DLBCLs biopsies

RNA ISH was performed on DLBCL FFPE biopsies, sectioned for no more than 2 months, using RNAscope® 2.5 HD Reagent RED Kit (Cat no. 322350, Advanced Cell Diagnostics (ACD) Hayward, CA) in 2 days (see the workflow in Fig. 1).

In the first day, the sections were deparaffinized by heating slides at 60 °C for 1 h in the HybEZTM Oven (Cat no. 310010), and subsequently by dipping the slides in fresh xylene, two times for 5 min each, working in a fume hood with the staining dish. Afterwards, sections were dehydrated in fresh 100% ethanol, two times for 1 min, working in a fume hood with the staining dish. The sections were then air dried for at least 1 h at room temperature (RT) until they were completely dried to facilitate the target retrieval. During this break to save time, Target Retrieval Reagent (TRR) (Cat no. 322000, ACD), wash buffer (WB) (Cat No. 310091, ACD), Gill's I hematoxylin solution (Cat. no. 1 GHS132, Sigma-Aldrich, Merck KGaA, Darmstadt, Germany) and ammonia water (Cat. no. 30501, Honeywell, Fluka) were prepared: for 1 × TRR, were added 70 ml of 10 × TRR concentrate to 630 ml of distilled water; for 1 × WB, were added 60 ml of 50 × WB concentrate, pre-warmed at 40 °C for 30 min, to 2.94 l of distilled water; Gill's I hematoxylin solution were filtered with 0.22 µm pore size syringe filter and stored at RT protected from light; for 0.02% ammonia water solution, were added 1.43 ml of 1 N ammonium hydroxide solution to 250 ml of distilled water. After drying, the sections were incubated with three drops of hydrogen peroxide (pretreat-1 solution) for 10 min in the dark to block endogenous peroxidase activity. From this passage onwards, where the number of drops of specific solutions will be indicated, it should be remembered that the sections were covered with coverslips to favor the diffusion of the specified solutions and to lower the kit costs (1 kit is usually sufficient to process 20 sections, but with coverslips, the yield can be doubled). After the sections were washed in distilled water two times for 1 min, balanced in boiling distilled water for 10 s (sec) and immersed in TRR (pretreat-2 solution) for 15 min at 98-102 °C using a heating plate (it is possible to recycle the same TRR twice without affecting the results). Later, the sections were washed in distilled water two times for 1 min, dehydrated in 100% ethanol for 1 min and air dried for at least 1 h at RT. Finally, a hydrophobic barrier was created with ImmEdge Hydrophobic Barrier Pen (Cat. no. 310018, ACD) and the sections were left overnight at RT to facilitate the barrier drying.

In the second day, the HybEZ™ Oven was turned on at 40 °C for at least 30 min, a humidifying paper wet with 50 ml of distilled water was placed in the HybEZ™ Control Tray to avoid excessive evaporation during probes and AMP1-6 incubation. The reagents AMP1–6 from the detection kit were kept at RT, the probes were pre-warmed at 40 °C for at least 10 min in a water bath, and the Glycergel Mounting media were kept at 40 °C until slides were mounted. After this first preparatory phase, the sections were incubated with two drops of protease (pretreat-3 solution; Cat no. 322331, ACD) to provide better access to RNA target, for 30 min at 40 °C using the HybEZ™ Oven (Cat no. 310010, ACD) (this oven was used in all subsequent steps where the incubation temperature is higher than the RT, because it avoids excessive evaporation and keeps the temperature constant). The slides were then washed twice in distilled water and hybridized with two drops of Hs-STAT3 (Cat no. 425631, ACD), or dapB (Cat No. 310043, ACD), or Hs-PPIB (Cat no. 313901, ACD) probes for 2 h at 40 °C, washed in WB two times for 2 min each (hereinafter referred to as WB 2 × 2), incubated with two drops of AMP-1 (all the AMP are from the Detection kit, Cat no. 322360, ACD) for 30 min at 40 °C, washed in WB 2 × 2, incubated with two drops of AMP-2 for 15 min at 40 °C, washed in WB 2 × 2, incubated with two drops of AMP-3 for 30 min at 40 °C, washed in WB 2 × 2, incubated with two drops of AMP-4 for 15 min at 40 °C, washed in WB 2 × 2, incubated with two drops of AMP-5 for 30 min at RT, washed in WB 2 × 2, incubated with two drops of AMP-6 for 15 min at RT, and washed in WB 2 × 2. Keeping the sections in WB, the Fast-RED (Cat no. 322360, ACD) was prepared, mixing 1 µl of Fast-RED A with 60 µl of Fast-RED B, and 61 µl of this mixture was used for one section for 10 min at RT. After washing under flowing tap water for 2 min, the sections were counterstained with Gill's I hematoxylin for 2 min (directly placed on the sections and not by immersion), washed under flowing tap water for 2 min, immersed in bluing reagent 0.02% ammonia water for 30 s, washed under flowing tap water for 2 min and finally mounted with Glycergel Mounting media (Cat. no. C0563, Agilent Dako, Santa Clara, CA).

The sections were then examined with an Olympus photomicroscope (Olympus Italia, Rozzano, Italy) to evaluate the probe's red spot signals and subsequently intended to images acquisition or to dual ISH–IHC processing.

RNAscope ISH slide scanning and analysis

Sections were scanned using the whole-slide morphometric analysis scanning platform Aperio ScanScope CS (Leica Biosystems, Nussloch, Germany) at 40× magnification and stored as digital high-resolution images on the workstation associated with the instrument. Fast-RED semi-quantitative image analysis was performed on ten randomly selected fields observed at 40× magnification using the color deconvolution plugin for Fiji ImageJ (for more details see "Using ImageJ to analyze RNAscope® and Base ScopeTM data, ref. TS 46-003, on https://acdbio.com/). Briefly, the TIFF section images were commuted

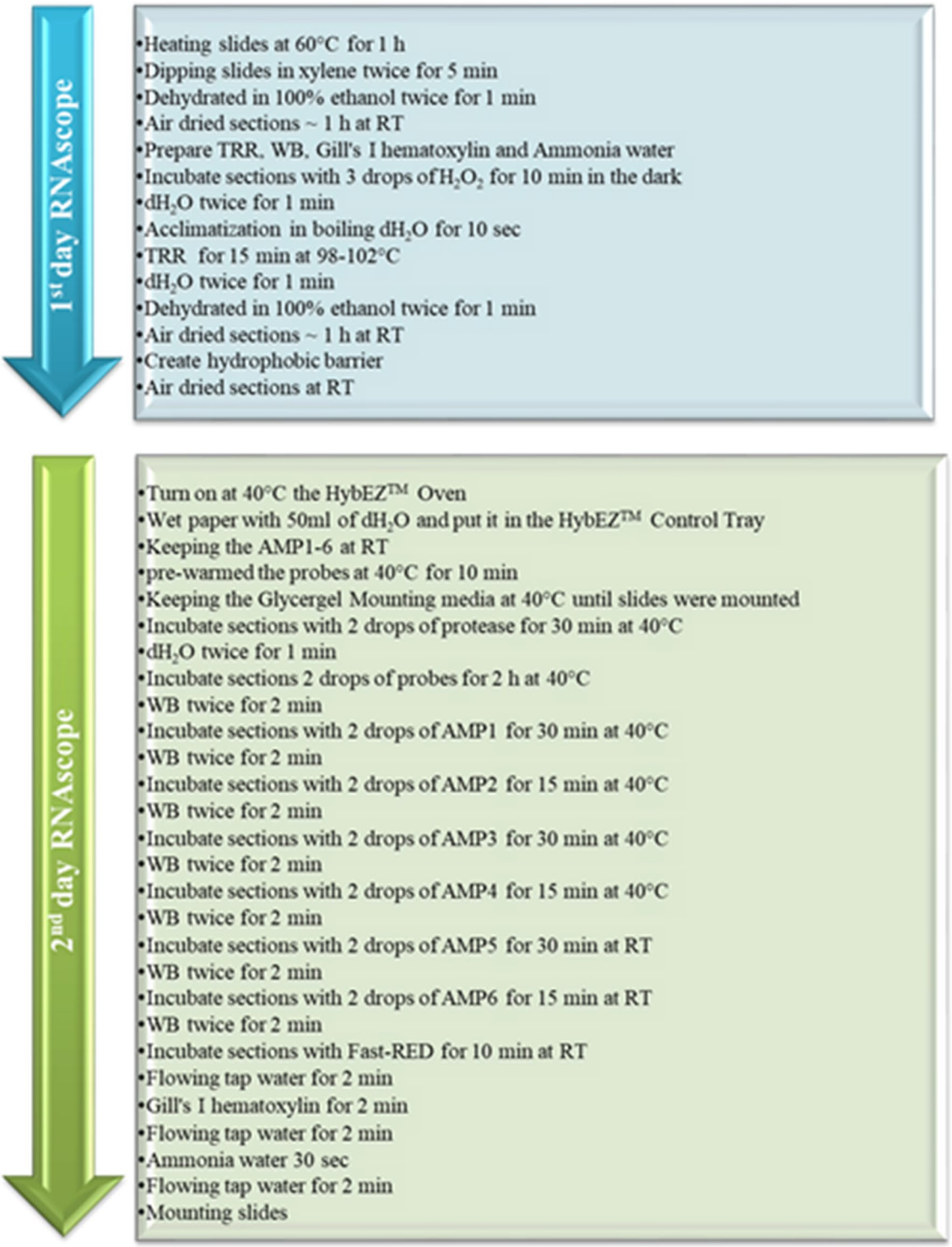

Fig. 1 RNAscope workflow illustration. The RNAscope protocol for DLBCLs biopsies is divided in 2 days. In the first day, the major steps are the deparaffinization and the pretreatment with TRR for which to reach the specified temperature interval is a crucial step. In the second day, the major steps are the protease pretreatment, target probe hybridization, signal amplification and signal detection. In the second day, it is crucial to pay attention to the different steps at RT or at 40 °C, and is important to work in a humidifying chamber

in jpag format with paint software, open in Fiji ImageJ, deconvoluted by Color Deconvolution by ROI function to obtain single-channel-splitted images. The Fast-RED-splitted images for probes and hematoxylin ones for nuclei were analyzed by Trainable Weka Segmentation plugin, adjusted for the threshold and evaluated by the analyze particle function to define the number of probes per nuclei (Fig. 2). The mRNA expression was assessed as number of Fast-RED-positive probes. Results are given as mean ± SD.

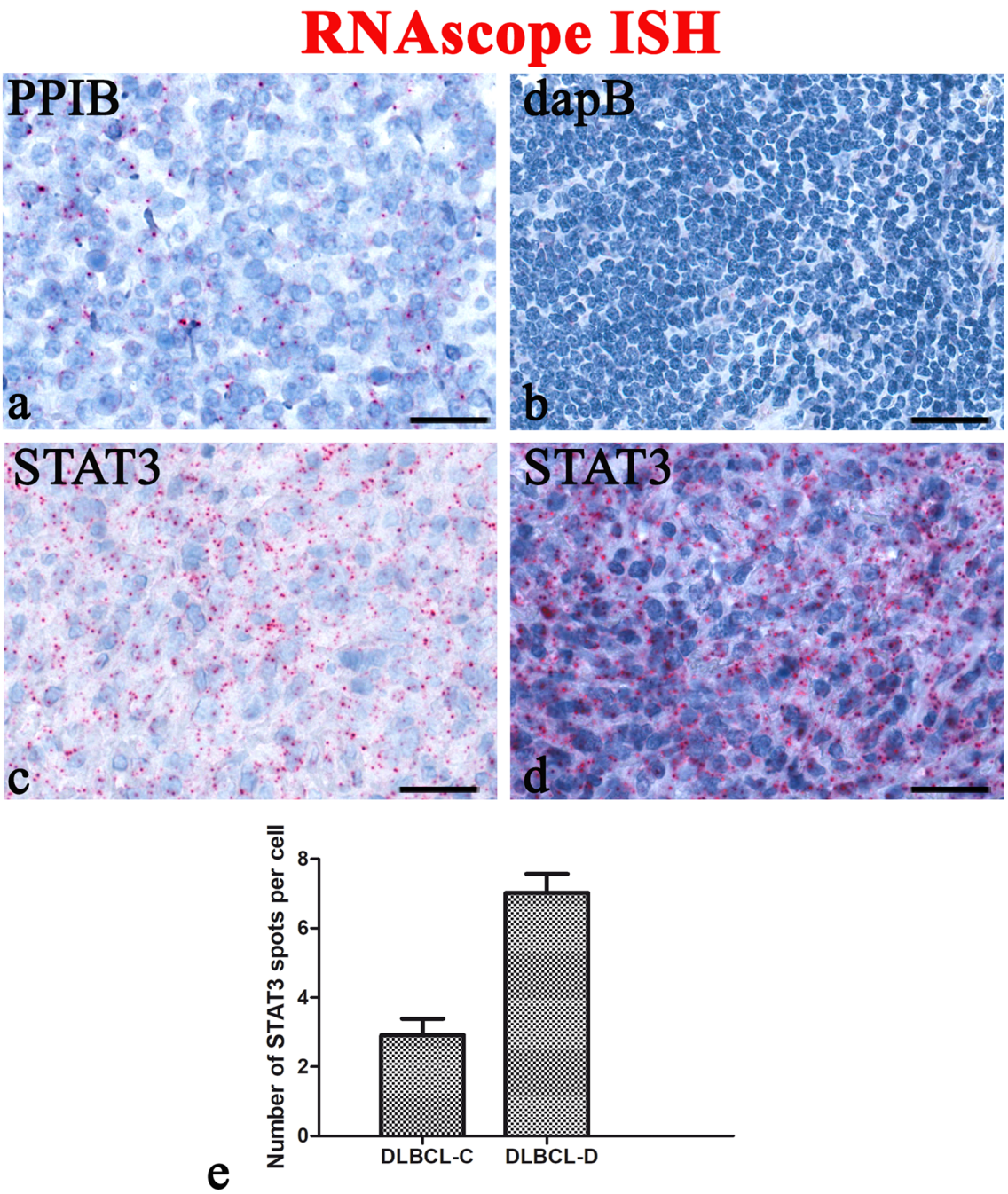

Fig. 2 RNAscope STAT3 mRNA expression in DLBCLs biopsies. The RNAscope assay on DLBCLs biopsies shows the positivity for PPIB (a housekeeping gene coding for peptidylprolyl isomerase B) (**a**) and the negativity for dapB (a bacterial gene coding for dihydrodipicolinate reductase) (**a**) resulting in a good mRNA quality. STAT3 mRNA expression in two DLBCLs biopsies (**c**, **d**) is quantify as number of spots per cell as shown in the histogram (**e**). Number of STAT3 red spots per cell is 2.91 ± 0.48 in **c** and 7.02 ± 0.55 in **d**. Scale bar **a**–**d** 60 µm

STAT3/FVIII dual RNAscope ISH–IHC

After the bright-field microscope examination, the same DLBCLs sections used for RNAscope assay, since Fast-RED produces a red signal detectable in bright-field and fluorescent microscopy, were undergo to immunofluorescence reaction for FVIII protein detection.

The coverslip was removed immersing the slides in distilled water in an oven at 60 °C. After several washing in PBS, the slides were kept 2 h in a blocking buffer [BB; P S pH 7.4 + 1% bovine serum albumin (BSA) + 10% normal goat serum (NGS)]; afterwards, the sections were exposed to rabbit anti-FVIII antibody (diluted 1:50; Cat. no. A0082, Agilent Dako, Santa Clara, USA) overnight at room temperature, followed by secondary antibody goat anti-rabbit Alexa-fluor 488 (Cat. no. R37116, Invitrogen, Carlsbad, CA, USA) diluted 1:300 in PBS for 2 h. After counterstaining with 0.01% TO-PRO-3 (Invitrogen) for 20 min for nuclear staining, slides were mounted with Vectashield® Antifade Mounting Medium. As controls, the primary antibody was omitted. The sections were examined under a Leica TCS SP2 (Leica, Wetzlar, Germany) confocal laser scanning microscope using 40 × and 63 × objective lenses with either 1 × or 2 × zoom factors (Fig. 3). A sequential scan procedure was applied during image acquisition and confocal images were taken at 0.2 µm intervals through the *z*-axis of the section. Images from individual optical planes and multiple serial optical sections were analyzed, digitally recorded and stored as TIFF files using Adobe Photoshop software (Adobe Systems).

Statistical analysis

Statistical significance of STAT3 mRNA expression in DLBCLs biopsies was performed using one-way ANOVA analysis and Bonferroni post hoc tests to compare replicate with GraphPad Prism 5.01 (GraphPad Software, SanDiego, CA, USA) and $p < 0.05$ was considered as the limit for statistical significance.

Results and discussion

It is well established that the oncogene STAT3 is constitutively over-expressed, active and is associated with a poorer prognosis in DLBCLs (Ding et al. 2008; Wu et al. 2011). It is a crucial component of the JAK/STAT signaling pathway required in many processes such as inflammation, immune suppression, and tumorigenesis by regulating the expression of various target genes, including cell-cycle regulators, angiogenic and apoptotic factors (Wake et al. 2015). In this work, to better understand the role of STAT3 in angiogenesis during DLBCLs and by the means of RNAscope technology, we showed that STAT3 mRNA is abundantly (at least more than two STAT3 molecules per cell) expressed in DLBCLs, but there is also a considerable heterogeneity between different patients. In fact, the semi-quantitative STAT3 mRNA expression analysis, as number of red spots per cell, in the two representative DLBCL patients, indicated as DLBCL-C and -D, showed that the number of STAT3 spots per cell could fluctuate a lot (Fig. 2 data expressed as mean ± SD: 2.91 ± 0.48 in C and 7.02 ± 0.55 in D). Furthermore, we showed that tumor vessels are delimited by cells double positive to both endothelial cell marker FVIII and the pleiotropic STAT3 indicating vasculogenesis as one of the possible angiogenesis mechanism that occurring in DLBCLs (Ruggieri et al. 2017; Tamma et al. 2019). STAT3 expression on DLBCLs endothelial cells could be represented an important indication for the personalized antiangiogenic therapy considering the individual patient features.

Neoangiogenesis has a main role on cancer progression, so much so that it was established as a hallmark of tumor growth and it can arise in a variety of forms such as sprouting angiogenesis, intussusceptive angiogenesis, vascular co-option, vasculogenic mimicry, postnatal vasculogenesis, and by the differentiation of putative cancer stem cells into endothelial cells (Ribatti 2014; Annese et al., 2019). In the same tumor, all these alternative mechanisms

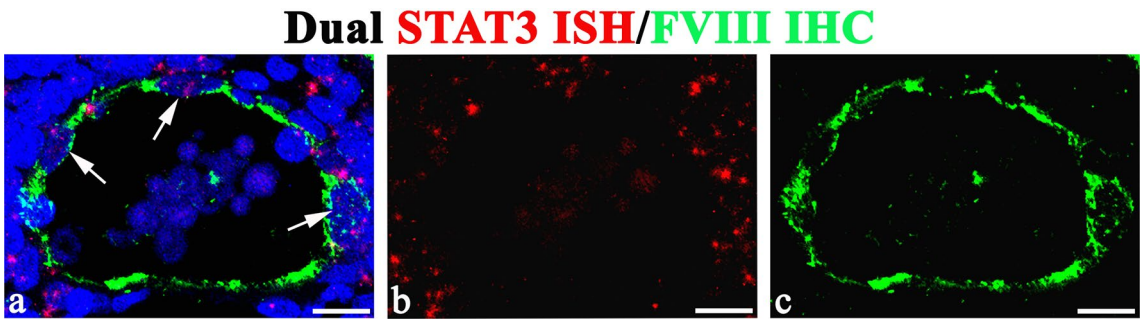

Fig. 3 STAT3 dual IHC/FVIII IHC confocal microscopy. Confocal fluorescence evaluation of dual STAT3 mRNA (**a**, **b** red spots) and FVIII protein (**a**, **c** green signal) in DLBCLs biopsies show a tumor vessels lined by $STATA3^{+}/FVIII^{+}$ endothelial cells (arrows). Scale bar **a**–**c** 10 µm

could occur simultaneously or as an alternative way to the main mechanisms making conventional antiangiogenic therapies, such as Bevacizumab, ineffective (Bottos and Bardelli 2013). Moreover, the antiangiogenic therapy could be ineffective, because the angiogenesis mechanisms active during tumor could be different, depending on the stage of the tumor progression or because the new vasculature is aberrant with a suboptimal perfusion (Bottos and Bardelli 2013).

Mutation or amplification of oncogenes, and inactivation or deletion of oncosuppressor genes can drive tumorigenesis directly promoting cancer cell proliferation and survival, and indirectly influencing the tumor microenvironment. This plays a fundamental role in supporting tumor growth and resistance to antiangiogenic therapy (Roma-Rodrigues et al. 2019). STAT3 can directly stimulate angiogenesis acting on endothelial cells (sprouting angiogenesis) or indirectly acting on inflammatory cell recruitment, as recently demonstrated for $CD163^+$ tumor-associated macrophages (TAM) and $CD8^+$ T-lymphocytes (Tamma et al., 2019). This suggests that the oncogenes' inhibition could have a double effect on cancer cells and on tumor microenvironment restoring a normal and functional vasculature and blocking the specific angiogenic mechanism activated by individual tumors (Bottos and Bardelli 2013). For example, in a preclinical model of squamous cell carcinoma, by endothelial cell tube formation in vitro and by a murine tumor xenograft models, it was demonstrated that STAT3 decoy oligonucleotide inhibits tumor angiogenesis targeting both the tumor cells and vascular compartments (Klein et al. 2014).

In such a context, where tumors are highly various in the different progression stage and patients are heterogeneous in terms of phenotype and treatment response, new approaches to study specific patients' features are needed. RNAscope dual ISH–IHC technology could be one of the most diffuse techniques for observing neoangiogenesis on tumors at single-vessel cell resolution. The evaluation of mRNAs and proteins on the same tissue section, keeping the morphological context usually missing in conventional techniques, is difficult and time consuming with classical single methods, such as real-time PCR and western blotting with mRNAs/proteins extracted from FFPE tissues, especially in case of precious human samples. The yield of classical techniques on FFPE tissues is very low in terms of quantity of total mRNAs/proteins and, therefore, the possibilities of investigation for multiple mRNA/protein targets on the same sample are reduced. Furthermore, these techniques are prone to interference from other types of unwanted cells, such as non-tumor cells, and from other unwanted tissue elements, such as fibrosis and necrosis.

Most pathologists preferred immunohistochemistry-based techniques, because are rapid and relatively inexpensive methods, allowing the simultaneous evaluation of a staining pattern, tissue architecture and tumor cells. Potentially, RNAscope dual ISH–IHC can be interpreted with fewer malignant cells than are needed for successful interpretation by fluorescence in situ hybridization (FISH) or other molecular technologies, usually used to evaluate aberrant gene expression in tumor.

Indeed, to simplify the standard in situ hybridization protocols, we provided a detailed one about reagents and equipment required, RNAscope and RNAscope dual ISH–IHC procedures, and how to scan and analyze the slides. We recommend the free Trainable Weka Segmentation plugin to successfully semi-quantify the number of spots per cell allowing an economic image processing and analysis to reduce the costs compared to the paid semi-quantitative counting software such as HALO™ software system from Indica Labs. A potential limitation of this plugin is the impossibility to classified the cells with a scoring methodology based on ACD scoring criteria (see https://acdbio.com/technical-support/solutions). This because the human eyes do not have such a high resolution to distinguish the individual spots joined in clusters. Moreover, it would be excessively laborious to perform manual calculations considering the single probe signal intensity for each cell.

Overall, we suggest that combining ultrasensitive RNAscope ISH with standard IHC on FFPE sections will prove to be an important technique in the oncology fields. A detailed knowledge of the main tumor angiogenic dynamics that take place in DLBCLs will provide new insights that are essential for clarifying which subgroup of patients will really benefit of antiangiogenic therapy as part of first-line treatment or in a relapsed/refractory setting.

Acknowledgements This work was supported by Fellowship Fondazione Italiana per la Ricerca sul Cancro e Associazione Italia per la Ricerca sul Cancro (FIRC-AIRC) 1-year fellowship "Laura Bassi" id. 20879 to TA. Associazione "Il Sorriso di Antonio, Corato, Italy, is also acknowledged.

Author contributions TA wrote the manuscript with support from RT and SR; TA and MD developed the protocol; EM, GS, and DR supervised the manuscript.

Compliance with ethical standards

Conflict of interest All authors declare the absence of conflict of interest.

References

Annese T, Tamma R, Ruggieri S, Ribatti D (2019) Erythropoietin in tumor angiogenesis. Exp Cell Res 374:266–273. https://doi.org/10.1016/j.yexcr.2018.12.013

Bottos A, Bardelli A (2013) Oncogenes and angiogenesis: a way to personalize anti-angiogenic therapy? Cell Mol Life Sci 70(21):4131–4140. https://doi.org/10.1007/s00018-013-1331-3

Cacciatore M, Guarnotta C, Calvaruso M, Sangaletti S, Florena AM, Franco V, Colombo MP, Tripodo C (2012) Microenvironment-centred dynamics in aggressive B-cell lymphomas. Adv Hematol 2012:138079. https://doi.org/10.1155/2012/138079

Coiffier B, Sarkozy C (2016) Diffuse large B-cell lymphoma: R-CHOP failure-what to do? Hematol Am Soc Hematol Educ Program 2016:366–378. https://doi.org/10.1182/asheducation-2016.1.366

Ding BB, Yu JJ, Yu RY, Mendez LM, Shaknovich R, Zhang Y, Cattoretti G, Ye BH (2008) Constitutively activated STAT3 promotes cell proliferation and survival in the activated B-cell subtype of diffuse large B-cell lymphomas. Blood 111:1515–1523. https://doi.org/10.1182/blood-2007-04-087734

Feugier P, Van Hoof A, Sebban C, Solal-Celigny P, Bouabdallah R, Ferme C, Christian B, Lepage E, Tilly H, Morschhauser F, Gaulard P, Salles G, Bosly A, Gisselbrecht C, Reyes F, Coiffier B (2005) Long-term results of the R-CHOP study in the treatment of elderly patients with diffuse large B-cell lymphoma: a study by the Groupe d'Etude des Lymphomes de l'Adulte. J Clin Oncol 23:4117–4126. https://doi.org/10.1200/JCO.2005.09.131

Friedberg JW (2011) Relapsed/refractory diffuse large B-cell lymphoma. Hematol Am Soc Hematol Educ Program 2011:498–505. https://doi.org/10.1182/asheducation-2011.1.498

Jaffe ES, Harris NL, Stein H, Isaacson PG (2008) Classification of lymphoid neoplasms: the microscope as a tool for disease discovery. Blood 112:4384–4399. https://doi.org/10.1182/blood-2008-07-077982

Khosravi Shahi P, Perez Manga G (2006) Diffuse large B-cell lymphoma. Med Clin 127(1):17–21

Klein JD, Sano D, Sen M, Myers JN, Grandis JR, Kim S (2014) STAT3 oligonucleotide inhibits tumor angiogenesis in preclinical models of squamous cell carcinoma. PLoS One 9:e81819. https://doi.org/10.1371/journal.pone.0081819 **(eCollection 2014)**

Pan YR, Chen CC, Chan YT, Wang HJ, Chien FT, Chen YL, Liu JL, Yang MH (2018) STAT3-coordinated migration facilitates the dissemination of diffuse large B-cell lymphomas. Nat Commun 9(1):3696. https://doi.org/10.1038/s41467-018-06134-z

Ribatti D (2014) History of research on angiogenesis. Chem Immunol Allergy 99:1–14. https://doi.org/10.1159/000353311

Ribatti D, Nico B, Ranieri G, Specchia G, Vacca A (2013) The role of angiogenesis in human non-Hodgkin lymphomas. Neoplasia 15:231–238

Roma-Rodrigues C, Mendes R, Baptista PV, Fernandes AR (2019) Targeting tumor microenvironment for cancer therapy. Int J Mol Sci. https://doi.org/10.3390/ijms20040840

Ruggieri S, Tamma R, Resta N, Albano F, Coccaro N, Loconte D, Annese T, Errede M, Specchia G, Senetta R, Cassoni P, Ribatti D, Nico B (2017) Stat3-positive tumor cells contribute to vessels neoformation in primary central nervous system lymphoma. Oncotarget 8:31254–31269. https://doi.org/10.18632/oncotarget.16115

Tamma R, Ingravallo G, Albano F, Gaudio F, Annese T, Ruggieri S, Lorusso L, Errede M, Maiorano E, Specchia G, Ribatti D (2019) STAT-3 RNAscope determination in human diffuse large B-cell lymphoma. Transl Oncol 12:545–549. https://doi.org/10.1016/j.tranon.2018.12.008

Ungefroren H, Sebens S, Seidl D, Lehnert H, Hass R (2011) Interaction of tumor cells with the microenvironment. Cell Commun Signal 9:18. https://doi.org/10.1186/1478-811X-9-18

Wake MS, Watson CJ (2015) STAT3 the oncogene – still eluding therapy? FEBS J 282:2600–2611. https://doi.org/10.1111/febs.13285

Wang F, Flanagan J, Su N, Wang LC, Bui S, Nielson A, Wu X, Vo HT, Ma XJ, Luo Y (2012) RNAscope: a novel in situ RNA analysis platform for formalin-fixed, paraffin-embedded tissues. J Mol Diagn 14:22–29. https://doi.org/10.1016/j.jmoldx.2011.08.002

Wu ZL, Song YQ, Shi YF, Zhu J (2011) High nuclear expression of STAT3 is associated with unfavorable prognosis in diffuse large B-cell lymphoma. J Hematol Oncol 4:31. https://doi.org/10.1186/1756-8722-4-31